한국기계가공학회지, 제20권, 제7호, pp. 8～14(2021.07) ISSN 1598-6721(Print)
Journal of the Korean Society of Manufacturing Process Engineers, Vol. 20, No. 7, pp. 8~14(2021.07) ISSN 2288-0771(Online)

https://doi.org/10.14775/ksmpe.2021.20.07.008

Fracture Toughness Comparison of Weld Metal and Heat-Affected Zone of Brittle Crack Arrest Steel Welding Joint

Kyung-Shin Choi*, Seok-Hwan Kong*, Sang-Seok Seol*, Won-Jee Chung*,#
*Department of Mechanical Design Engineering, Changwon National University

후물재 용접부의 용착금속과 열영향부의 파괴 인성 비교 연구

최경신*, 공석환*, 설상석*, 정원지*,#
*국립창원대학교 기계공학부

(Received 05 April 2021; received in revised form 04 May 2021; accepted 14 May 2021)

ABSTRACT

Even welds that have passed non-destructive testing in the case of brittle crack arrest steel materials will actually have very fine weld defects. Based on studies showing that these defects adversely affect the structure if subjected to a certain period of load, the following conclusions were obtained by conducting CTOD tests on welding joints of high-strength BCA materials, structures comprising the upper decks of a large container vessel. First of all, the fatigue pre-cracking in the weld metal and heat affected areas was tested and the behavior was identified. Both parts of the welding joint are allowable range for the class regulations. In addition, CTOD results showed that the CTOD value in the heat affected area was more than 0.5 times higher than in the weld metal area.

Key Words : BCA(Brittle Crack Arrest), CTOD(Crack Tip Opening Displacement), Weld-Metal(용착 금속), Heat-affected Zone(열 영향부), Stress Intensity Factor(응력 확대 계수)

1. Introduction

The increase in global shipping traffic has inevitably entailed the construction of larger ships. It is necessary to lighten the structural weight of ships and improve their productivity by using high-strength steel materials. In particular, for large container ships, steel with a thickness of 80–100[mm] is used to ensure sufficient longitudinal strength.

These is referred to as thick steel plates or extremely thick steel plates. Due to the characteristics of the steel, several problems such as brittle fracture can be caused by the thickness of the plates. The thickness effect means that the patterns of failure appear differently depending on the thickness of the steel materials, even for the same material with the same properties. Distribution patterns of stress generated inside the material are classified as planar stress or planar deformation. For thinner plates, the

Corresponding Author :wjchung@chanwon.ac.kr
Tel: +82-55-213-3624, Fax: +82-55-263-5221

steel is gradually destroyed by plastic deformation due to external forces. In the case of thick steel plates or extremely thick steel plates, deformation is difficult due to the thickness. The disadvantage is that the destruction proceeds rapidly once a certain limit is reached. In addition to these disadvantages, studies have been conducted on fracture toughness through CTOD tests, such as excessive heat input, which also affects brittle fracture.[1] In addition, research on cooling speed, the effects of tissue, and alloy elements has also been carried out, but does not generally replicate the welding conditions in the field.[2-7] It is therefore urgent to be able to determine welding integrity because verification is not performed at the locations where the welding takes place.

In this study, behavior patterns that affect the change in the heat input and fracture toughness for the welding joints of thick steel material used in large container ships were investigated.

2. Experiment method

2.1 Mechanical and chemical properties

The steel materials used in this study were EH-40 BCA (Brittle Crack Arrest) with a thickness of 80[mm], which was applied to the upper deck of the container ship using a thermo-mechanical controlled process (TMCP). Table 1 shows the chemical composition, and Table 2 lists the mechanical properties.

Table 1 Chemical composition of EH40-BCA steel

Steels		C	Si	Mn	P	S	S-Al	Ceq	Pcm
TMCP	80 mm	0.06	0.13	1.68	0.006	0.0013	0.038	0.43	0.18

Ceq=C+Mn/6+(Ni+Cu)/15+(Cr+Mo+V)/5
Pcm(%)=C+Si/30+Mn/20+Cu/20+Ni/60+Cr/20+Mo/15+V/10+5B

Table 2 Mechanical properties of EH40-BCA steel

Steels	Yield Stress (MPa)	Tensile Strength(MPa)	Elongation (%)
EH40BCA-TMCP-80mm	507	598	24

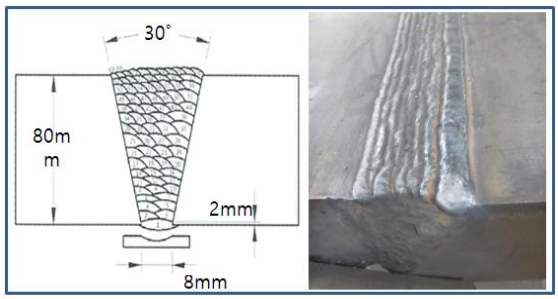

Fig. 1 Detail of welding joint FCAW

The mechanical properties of the applied steel materials needed to be suitable for high-strength welding with a yield strength of 470[MPa]. A flux core wire corresponding to the E81T-C1A6-K2 standard of the American Welding Society (AWS A5.36), was manufactured with a wire diameter of 1.4[mm] and 99.9% CO_2 was used as a protective gas.

2.2 Welding method

The welding improvement shape is shown in Fig. 1 to compare and evaluate the fracture toughness of the weld metal according to the FCAW welding technique for thick steel material.

The steel materials consisted of thick quenched and tempered steel. In the case of the initial bead, the maximum heat input was 55[kJ/cm] it was subsequently maintained at 34.4[kJ/cm]. The following measurements were used: groove angle 30°, root face 0–3[mm], root gap 3–8[mm]. The preheating temperature and maximum interlayer temperature were 127[°C] and 170[°C], respectively, following the FCAW technique, and the welding conditions are listed in Table 3.

Table 3 Summary of the welding parameters

Welding Process	Current (A)	Voltage (V)	Travel Speed (cm/min)
FCAW	290	33	48
SAW	880	33	50

2.3 Fracture toughness test

If the steel material to be tested is thin, the plastic deformation caused by the yield phenomenon before the crack is formed cannot be measured. For this reason, in order to evaluate thick steel material where the plastic deformation cannot be ignored, CTOD, which is a parameter applicable to material that can exhibit nonlinear behavior, was used in this study. The notch of the CTOD specimen was at the center of the weld metal and in the heat-affected zone. Specimens were prepared so that the notch was in the direction of the welding. According to British Standard (BS) 7448 Part 1: 1991, pre-cracking measured the fatigue crack length on one specimen as an actual value, which was derived from Equation (1). The actual crack length[mm] was calculated as the sum of the machining notch length [mm] and fatigue crack length[mm].

$$a_f = \frac{(a_f + a_{f8}) \times 0.5 + a_{f1} + a_{f2} + \cdots + a_{f7}}{8} \quad (1)$$

The fatigue crack length[mm] was measured at nine points to, located at a depth of 1% of the thickness from the surface and equally spaced between the two ends, as shown in Fig. 2. Excluding the end points, seven points from to were located at equal intervals inside the surface.

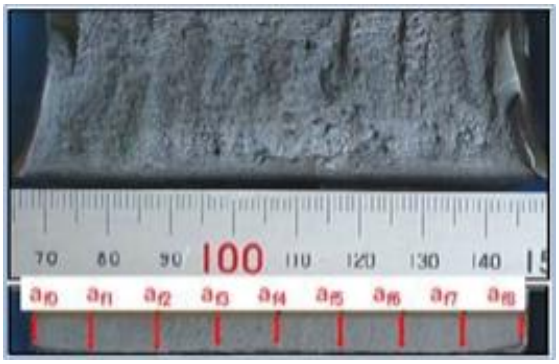

Fig. 2 Location of measuring point for specimen

The formula for calculating the fracture test for 0.2% proof temperature was derived from BS 7448 Part 2 : 1997, as shown in Equation (2)[8], where T is the test temperature, is the fatigue cracking temperature, and is the breaking test.

$$\sigma_Y = \sigma_{Y0} + \frac{10^5}{(491 + 1.8 \times T)} - 189 \quad (2)$$

The equipment used a three-point bending tester DYHU-1000[kN] Universal machine to select the type of failure determined in Annex Fig. 13 of 1991 (characteristic types of force versus displacement records in fracture test). A temperature of -10±2[°C] was maintained for 38.5[min] as a condition for tempering. A mixture of LN, alcohol, and dry ice was used as the cooling medium.

3. Experiment result

3.1 Fatigue pre-cracking and fracture toughness of weld metal

In performing a general fracture toughness test, measurement of the pre-crack length was omitted because the surface crack length of the specimen was measured in the calibration step.

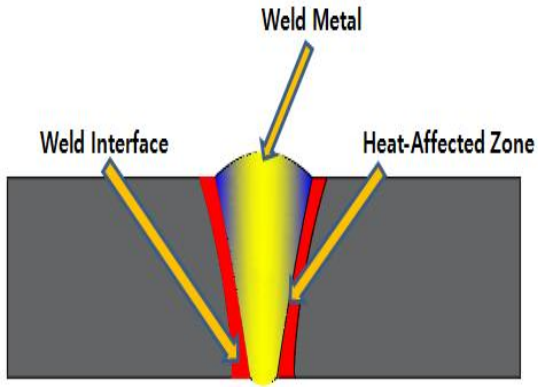

Fig. 3 Notch position of welding joint

Table 4 Fatigue pre-cracking parameters for weld metal

Parameters	Measured	Standard	Results
Max. fatigue pre-cracking force	75 kN	≦ 112	OK
Stress ratio	0.1	0～0.1	OK
Max. fatigue stress intensity factor	39	≦93	OK
Cyclic No (Cycles)	28959	-	-
$\Delta K/E(m^{1/2})$	0.000170	≦0.0003	OK

Table 5 Weld metal results for 9 crack length of the fatigue crack [Unit: mm]

Specimen	No.	Length [mm]	No.	Length [mm]
Original crack length	a_1	38.5	a_2	39.7
	a_3	39.3	a_4	39.2
	a_5	39.0	a_6	39.0
	a_7	39.7	a_8	40.0
	a_9	39.5	a_0	39.4
a_0/W	0.512	0.45~0.55		OK
Difference of each crack	0.037	Weld≦0.2		OK

However, in this study, fatigue cracking occurred and grew in tempered steel with a thickness of 80[mm] or more, and pre-fatigue crack measurement was performed in consideration of the tunneling effect. Fig. 3 shows the details of the notch position of the welding joint.

Table 4 shows the results of the fatigue pre-cracking parameters at the weld metal area.

To measure the maximum fatigue stress intensity factor range and the stress ratio, applied loads were set to a force of 75[kN] in plastic deformation, using a stress ratio of 0.1, and a frequency of 10[Hz] in order to evaluate the effect of the frequency of the cyclic stress. The degree of influence related to whether or not cracks are formed was 151[MPa]. Table 5 shows the difference between the maximum and minimum values of the nine crack lengths.

3.2 Fatigue pre-cracking and fracture toughness in the heat-affected zone

In general, for high-stiffness steels, changes in strength, ductility, and toughness in the heat-affected zone showed different patterns from those of ordinary maximum and minimum values of the nine crack lengths. In the heat-affected zone, the overall strength was increased, but the area heated near the transformation point tended to have a lower strength than the base material. It showed the lowest ductility in the bond area, then recovered gradually and showed a higher peak value than the ductility of the base metal near the transformation point. It also had the characteristic of recovering to normal afterwards. The changes in toughness showed in the form of aging and embrittlement near the bond, where the grains were coarsened at transformation points. In addition, owing to the characteristics of the thick plate used in this study, the 2D flows were affected by the thickness and 3D heat flow state, where the plate thickness could be regarded as infinite. In 2D heat flow, defects such as torsion, deformation, and melting can occur because overheating occurs during welding. For this reason, pre-heating was performed before welding to slow down the cooling rate and prevent unnecessary embrittlement in the weld metal and heat-affected areas. The results of changing each variable of the fatigue pre-cracks in the heat-affected zone of the thick reinforced steel are also shown in Table 4.

The experiment was conducted under the same conditions as those used for the weld metal. The heat-affected zone also showed a similar pattern to the weld metal part, but the maximum stress factor, which is the degree of influence on the formation of cracks, was 156[MPa], which is slightly higher. Table 6 shows the maximum and minimum fatigue crack values obtained by measuring the crack length at nine equally spaced intervals.

Table 6 Heat-Affected Zone results for 9 crack length of the fatigue crack [Unit: mm]

Specimen	No.	Length [mm]	No.	Length[mm]
Original crack length	a_1	39.1	a_2	40.7
	a_3	40.1	a_4	39.3
	a_5	39.0	a_6	38.9
	a_7	38.9	a_8	39.3
	a_9	38.5	a_0	39.4
a_0/W	0.512	0.45~0.55		OK
Difference of each crack	0.055	Weld≦0.2		OK

3.3 Fracture toughness of weld metal and heat- affected zone

Fig. 4 shows the CTOD weld metal results. When the permanent displacement value of the notch is 3.27 [mm] and the maximum force is 291.5[kN], the CTOD is more than 1[mm].

There was no pop-in phenomenon, in which materials passed through the surrender store and showed a sudden drop in load and an increase in displacement. In this case, the mean values are prior to destruction at the local point of the initial crack shear. The change in crack length makes a difference in the binding force of the crack tip; therefore, even in the vicinity of the same weld, different results can be obtained depending. The CTOD results for the heat-affected zone are shown in Fig. 5. The curve indicated by the low-power regression line on the graph is the crack-resistance curve. This curve shows the area where the cracks are stable and no instability occurs. If the material is large, it can be seen by the slope of the curve that the resistance to propagation of the crack is high. Therefore, according to the slope curve, it is found to be an important characteristic value of the material.

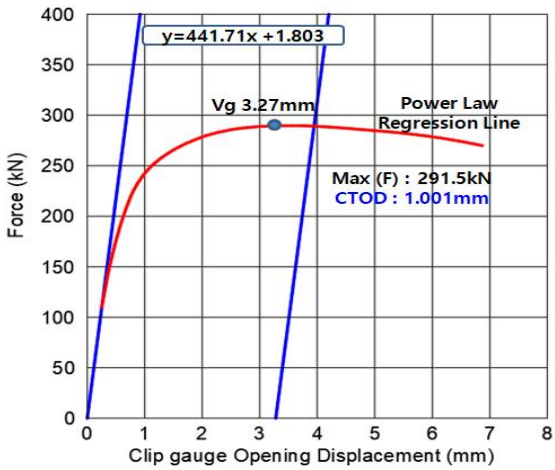

Fig. 4 Result of force and crack opening displacement for weld metal on the exact position

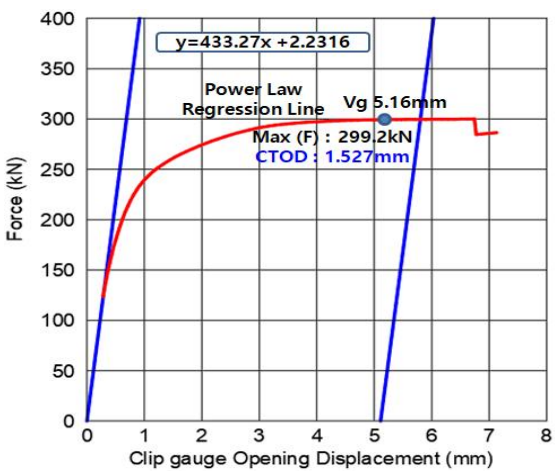

Fig. 5 Result of force and crack opening displacement for heat-affected zone

Table 7 Results for CTOD value

Weld type	V_g [mm]	Max force [kN]	CTOD [mm]
Weld metal	3.27	291.5	**1.001**
Heat-affected zone	5.16	299.2	**1.527**

During the test, the graph showed no unstable fracture, and the crack progressed relatively stably. Defining the maximum load at this time, the COTD value of the weld metal was 1.001[mm], and the CTOD value at the heat-affected zone was 1.527[mm]. Both welds largely satisfy the minimum CTOD requirement of 0.15[mm] of DNV and GL Classification Rules. However, it can be seen that the weld metal portion was significantly lower than the heat-affected portion. This is because the shape of the beveling at the welding joint and the force of shrinkage due to the binding or cooling of these shapes was affected. In particular, this experiment was conducted with the possibility of presence of a material that could cause defects, due to the accumulation of inclusions of microscopic foreign matter in the molten paper and slag generated during welding at the crack tip of each welding area. The final results of the fracture toughness in the weld metal and heat-affected zone are compared in Table 7.

4. Conclusion

In the case of thick steel plates and extremely thick steel plates, even welds that have passed non-destructive tests could still have very fine weld defects. Based on findings that show that these defects adversely affect the structure when a load is applied for a certain period of time, this study examined how high heat input affected each welding site at the welded joints of high-strength thick steel plate, which is a type of structure that constitutes the upper deck of a large container ship through fracture toughness tests, the following conclusions were obtained.

1. Both the weld metal part and the heat-affected part obtained weld integrity that satisfied the allowable ranges of the stress ratio and maximum fatigue stress expansion factor within the maximum applied load.
2. As a result of the displacement from the load cell and the clip gauge attached to the notch in the tester, it was confirmed that the material retained its original properties up to a displacement of 3.27[mm] in the weld metal part and 5.16[mm] in the heat-affected zone.
3. In the CTOD results, both welds showed satisfactory values within the range of the classification rules. It was found through experiments that the CTOD value was 0.5 times greater in the heat-affected zone than in the weld metal zone.

References

1. Shin, Y. T., Kang, S. W., Kim, M. H., "Evaluation of Fracture Toughness and Microstructure on FCA Weldment According to Heat Input," Journal of Welding and Joining, Vo1. 26, No. 3, pp. 51-60, 2008.
2. Glover, A. G. McGrath, J. T. Tinkler, M. J. and Weatherly, G. C., "The Influence of Cooling Rate and Composition on Weld Metal Microstructures in a C/Mn and a HSLA steel," Welding Journal, Vol. 56, No. 9, pp. 267-273, 1977.
3. Smith, N. J. Mcgrath, J. T. Gianetto, J.A. and Orr, R .F., "Microstructure/Mechanical Property Relationship of Submerged Arc Welds in HSLA 80 Steel," Welding Journal, Vol. 68, No. 3, pp. 112-120, 1989.
4. McGrath, J. T. and Gianetto, J. A., "Some Factors Affecting the Notch Toughness Properties of High Strength HY80 Weldments," The Canadian Journal of Metallurgy and Materials Science, Vol. 25, No. 4, pp. 349-356, 1986.
5. Evans, G. M., "The Effect of Nickel on Microstructure and Properties of C-Mn all Weld Metal Deposits," Welding Research Abroad, Vol. 1, No. 1, pp. 2-13, 1991.
6. Zhang, Z. and Farrar, R. A., "Influence of Mn and Ni on the Microstructure and Toughness of

C-Mn-Ni Weld Metals," Welding Journal, Vol. 76, No. 5, pp. 183-196, 1997.

7. Dallam, C. B. Liu, S. and Olson, D. L., "Flux Composition Dependence of Microstructure and Toughness of Submerged Arc HSLA Weldment," Welding Journal, Vol. 64, No. 5, pp. 140-151, 1985.
8. BS7448: Part 2 : 1997, "Fracture Mechanics Toughness Tests, Part 2. Method for the Determination of K_{IC}, Critical CTOD and Critical J Values of Welding in Metallic Materials," (British Standard)